Chemical Engineering Journal 160 (2010) 623–633

Contents lists available at ScienceDirect

Chemical Engineering Journal

journal homepage: www.elsevier.com/locate/cej

Vanadium loaded carbon-based monoliths for the on-board no reduction: Influence of temperature and period of the oxidation treatment

A. Boyano[a], C. Herrera[b], M.A. Larrubia[b], L.J. Alemany[b], R. Moliner[a], M.J. Lázaro[a,*]

[a] Instituto de Carboquímica, CSIC, c/. Miguel Luesma Castán, E-50018 Zaragoza, Spain
[b] Departamento de Ingeniería Química, Facultad de Ciencias, Campus de Teatinos s/n, Universidad de Málaga, E-29071 Málaga, Spain

ARTICLE INFO

Article history:
Received 2 December 2009
Received in revised form 29 March 2010
Accepted 31 March 2010

Keywords:
SCR
Carbon catalyst
Carbon oxidation

ABSTRACT

A carbon coated monolith was modified by different oxidative treatments to introduce different oxygen surface groups. Three kinds of liquid oxidizing agents (HNO_3, H_2SO_4 and H_2O_2) were used at different temperatures and residence times. The resulted oxidized activated carbon coatings were impregnated with 3% V wt on carbon and tested for the SCR of NO with NH_3 in a temperature range of 150–350 °C. The performance of the carbon coated catalysts was assessed by characterization of supports and catalysts through their textural and chemistry surface properties. In this sense, regarding the preparation of the catalysts, oxidation process plays itself a promoting role in the formation of oxygen surface groups that to a certain extent improves the catalytic activity. Inorganic acid, especially HNO_3 oxidation increases mainly the carboxyl and lactone groups whereas H_2O_2 oxidation significantly increases oxygen surface groups attributed to phenol, and carbonyl/quinine groups.

Generally, NO reduction activity is increased when fresh catalyst surface acidity increases and vanadium is doped on it. HNO_3 oxidized samples are able to fix higher amounts of vanadium in comparison to other oxidized monoliths. This fact can be attributed to the fact that the fresh catalyst surface acidity caused by the HNO_3 oxidation has a promoting role to favour well anchored and distributed vanadium onto its surface. Oxidation as well as vanadium impregnation process decrease BET surface area and micropore volume of supports. However, the chemistry surface developed for the oxidation process seems to be much more important promoting SCR activity and consequently a higher catalytic activity is observed for oxidized samples.

1. Introduction

High performance NO reduction techniques, especially for on-board applications, represents a current necessity for modern societies [1]. Today, increasingly stringent regulations require even more treatment of automotive effluents to maintain a better quality of air and atmosphere. Among the wide range of treatment technologies that are being developed and optimised, there are two that have gained the attention in the last years: the storage-reduction (NSR) [2,3] and the selective catalytic reduction (SCR) of NO_x [4,5]. Both technologies are prompt to be incorporated on-board diesel and lean-fuel vehicles to reduce the pollution caused. Among the various catalysts studied for the SCR of NO_x with NH_3 in the literature, activated carbon-based catalysts have been recently introduced in the SCR with very promising results [6]. The most remarkable characteristics of activated carbons are their high-surface area and porosity compared to other supports (Al_2O_3, TiO_2, CeO_2) and the presence of oxygen surface groups, which affects the catalytic activity [7]. Moreover, regarding SCR reaction carbon-based catalysts present two important advantages: they are active at lower temperatures [8] and show an activity promotion by SO_2 [9]. As a result, in this study they are proposed for the SCR on-board.

Liquid oxidation provides new opportunities for the creation of functional materials with different pore sizes and chemical functionalities [10,11]. In most cases, it is clear that both surface chemistry and pore structure of the catalytic material play a cooperative role in a specific application. In order to improve the performance of a catalyst, modifications of both properties, may be required. For increasing the number of surface functional groups on carbon materials, carbons are usually subjected to post treatments including oxidation, polymer coating and grafting [12–15]. Regarding surface modification of carbon-based porous materials, the most studied materials, are activated carbon and carbon nanotubes, within the purpose of achieving hydrophilic surface by the generation of a large number of oxygen-containing groups. In many cases the oxygen-containing groups behave as weak acids or bases, which possess ion-exchange properties. The acidic groups such as carboxyl, phenolic hydroxyl, lactone and quinone are introduced

* Corresponding author. Tel.: +34 976733977; fax: +34 976733318.
E-mail address: mlazaro@icb.csic.es (M.J. Lázaro).

1385-8947/$ – see front matter © 2010 Elsevier B.V. All rights reserved.
doi:10.1016/j.cej.2010.03.086

to achieve carbons treated with different properties [16–18]. Those formed surface complexes provide a new surface chemistry, which is reflected in the improved properties when carbon material is used as catalyst (support) [19–21].

Oxidation treatment is the most frequently used method, generally involving dry or wet oxidation, plasma treatment and electrochemical modifications. In the case of dry oxidation, gaseous oxidation agents like oxygen, ozone and carbon dioxide are often used [22]. Wet chemical oxidation involves the uses of nitric acid, sulphuric acid, phosphoric acid, alone or in combination with hydrogen peroxide, sodium hypochlorite, permanganese, chromate or dichromate of potassium, transition metal nitrates, etc. [23–25]. Saha et al. [26] studied oxidized porous activated carbons with nitric acid and distilled water at a ratio 1:1 (v/v) for 6 h at 90 °C, producing samples with weakly acidic functional groups. Pradhan et al. [27] functionalized activated carbons with surface oxygen complexes through oxidants like HNO_3 (1N), H_2O_2 and saturated solution of $(NH_4)_2S_2O_8$ in H_2SO_4 (8N). According to these authors nitric acid treatment is the most effective one in terms of modifying surface area and porosity of activated carbons. By comparing the chemically modified activated carbons with nitric acid and hypochlorite, Vinke et al. [12] stated, nitric acid oxidation is the most effective resulting the highest amount of acidic surface groups, whereas hypochlorite seems to be a much weaker oxidant.

Our previous study demonstrated that pore structure of activated carbon coated monoliths was partially destroyed in the presence of a liquid oxidant, reflecting some differences of reactivity depending on the nature of liquid oxidants under the same conditions (room temperature and for 24 h) [29]. In this study, we continue to investigate the oxidation behaviour of activated carbon coated monoliths to find out at which conditions a high amount of surface groups can be obtained, while maintaining the structural distribution and catalytic activity. In order to understand chemistry surface and structure evolution of activated carbon under determined oxidation processes, modified carbon coated monoliths were characterized by means of temperature programme desorption (TPD), thermogravimetric runs (TG), physisorption of N_2 at −196 °C, Raman and X-ray photoelectronic spectra (XPS). Our target is to reach a high active catalyst through a high-surface funcionalization of carbon surface but remaining its bimodal pore structure distribution.

2. Experimental

2.1. Support and catalyst preparation

Cordierite monoliths (400 cells per square inch (cpsi), 1 cm diameter and 5 cm length) were coated with a polymer blend by dip-coating method as described elsewhere [11]. Briefly, the monoliths were coated with the polymer, a blend of Furan resin and polyethylenglycol (2:1), carbonized at 700 °C and later on activated with CO_2 at 900 °C during 4 h to develop further surface area and porosity. The as-prepared carbon coated monoliths were treated with different oxidizing agents to develop surface oxygen complexes. For this purpose concentrated HNO_3, HNO_3 (2N), H_2SO_4 (2N) and H_2O_2 were applied. Sample preparation is summarised in Table 1. Subsequently, monoliths were thoroughly rinsed with distilled water and carefully dried.

All oxidized carbon coated monoliths were loaded with vanadium. The impregnation was carried out by ion-exchange method with an excess of solution of NH_4VO_3 until equilibrium. To facilitate the dilution of ammonium metavanadate ca. 5 mg of oxalic acid was added. Under these conditions, the pH of solution remains neutral and the solution holds a yellow colour indicative of the presence of VO^{2+} species. These monoliths were placed in a holder that was provided with a stirrer and contained 100 ml of the impregnating solution. This process was extended for 24 h until the equilibrium was reached. Subsequently, the monoliths were rinsed with distilled water, dried and thermally treated in N_2 at 350 °C.

Table 1
Short description of support preparation and nomenclature.

Support	Description
HNO_3 (c) 24 h Troom	Monolith oxidized with concentrated HNO_3 for 24 h at room temperature
HNO_3 (2N) 24 h Troom	Monolith oxidized with 2N HNO_3 for 24 h at room temperature
H_2SO_4 24 h Troom	Monolith oxidized with 2N H_2SO_4 for 24 h at room temperature
H_2O_2 24 h Troom	Monolith oxidized with H_2O_2 for 24 h at room temperature and
HNO_3 (c) 8 h Troom	Monolith oxidized with concentrated HNO_3 for 8 h at room temperature
HNO_3 (2N) 8 h Troom	Monolith oxidized with 2N HNO_3 for 8 h at room temperature
H_2SO_4 8 h Troom	Monolith oxidized with 2N H_2SO_4 for 8 h at room temperature
H_2O_2 8 h Troom	Monolith oxidized with H_2O_2 for 8 h at room temperature
HNO_3 (c) 8 h 80 °C	Monolith oxidized with concentrated HNO_3 for 8 h at 80 °C
HNO_3 (2N) 8 h 80 °C	Monolith, oxidized with 2N HNO_3 for 8 h at 80 °C
H_2SO_4 8 h 80 °C	Monolith oxidized with 2N H_2SO_4 for 8 h at 80 °C
H_2O_2 8 h 80 °C	Monolith oxidized with H_2O_2 for 8 h at 80 °C

2.2. Carbon support and catalyst characterization

The carbon-ceramic monolith supports were characterized regarding texture by N_2 physisorption and surface chemistry by temperature programmed desorption (TPD), thermogravimetric analysis (TGA), Raman and X-ray photoelectronic spectra (XPS). Catalysts were characterized by means of N_2 physisorption.

Nitrogen adsorption was performed on a Micromeritics ASAP 2020 at −196 °C. From the physisorption measurements with N_2, the specific surface area was calculated applying the BET equation. The *t*-plot method was applied to calculate the micropore volume whereas BJH method was used to calculate the parameters related to mesoporosity.

TPD measurements were carried out in a Micromeritics instruments. Before the TPD run, the sample was treated at 150 °C with 30 ml/min stream of He in order to release all physically adsorbed complexes. In the TPD, a temperature increase rate of 10 °C/min from 150 to 1050 °C was used. The CO_2 and CO evolved during the runs were detected by a gas chromatograph equipped with a thermal conductivity detector. TPD methods have become rather popular and in this work TPD peaks were attributed to specific surface groups following some trends summarised in [15]. In general, TPD spectra obtained with carbon materials show composite CO and CO_2 signals which must be deconvoluted before the surface composition can be estimated. The fitting response was carried out by a commercial computer program ORIGIN.

TGA runs were carried out in a CAHN TG 2151. After desorption at 100 °C for 20 min and the sample was heated up to 900 °C under air flow and a heating rate of 10 °C/min. This kind of experiments is really useful when samples would be exposed to high temperatures in the presence of O_2, since it gives information about the combustion resistance of supports.

Raman spectra were recorded on a Bruker-Senterra Raman imagine microscope with the 532 nm Nd-YAg laser and a CCD detector. Raman frequency was calibrated by a silicon slide. The laser was focused on the solid samples which were dispersed on microscope slides. Each spectrum was collected at room temperature under 10

Table 2
BET surface area and pore volumes of oxidized supports.

		$V_{micro\,total}$ (cm^3/g)	$V_{micro\,(<0.7\,nm)}$ (cm^3/g)	$V_{micro\,mediu}$ (cm^3/g)	$V_{mesopore}$ (cm^3/g)	S_{BET} (m^2/g)
	Activated	0.0172	0.0120	0.0052	0.0330	653
24 h room T°	HNO_3 2N	0.0186	0.0147	0.0049	0.0302	440
	HNO_3 (c)	0.0179	0.0159	0.0029	0.0269	364
	H_2SO_4 2N	0.0217	0.0109	0.0108	0.0305	650
	H_2O_2	0.0112	0.0076	0.0035	0.0308	616
8 h room T°	HNO_3 2N	0.0174	0.0141	0.0033	0.0263	404
	HNO_3 (c)	0.0065	0.0048	0.0017	0.0362	300
	H_2SO_4 2N	0.0119	0.0100	0.0019	0.0454	544
	H_2O_2	0.0161	0.0115	0.0046	0.0306	447
8 h 80 °C	HNO_3 2N	0.0165	0.0129	0.0036	0.0332	534
	HNO_3 (c)	0.0163	0.0118	0.0044	0.0280	552
	H_2SO_4 2N	0.0193	0.0140	0.0053	0.0196	515
	H_2O_2	0.0161	0.0114	0.0047	0.0344	537

mW of laser power. The experiments were performed in a dark environment to avoid interference from light and cosmic radiation.

Finally, *X-ray spectroscopy (XPS)* for the internal plates of monolith were acquired with a Physical Electronic 5700 spectrometer equipped with a hemispherical electron analyser and Mg Kα X-ray exciting source (1253.6 eV, 15 kV, 300 W). Samples were placed under vacuum (10^{-9} torr) and time of irradiation was minimized to avoid the metals reduction. It has been used as an internal patron for calibration Al_{2p} (73.9 eV) considering a deviation ±0.2 eV. As a consequence of the asymmetry presented by the signals, the bands are the result of the contribution of more than one species and the relative population has been determined by deconvolution. A strategy was developed for the mathematical deconvolution; in all cases the signal was adjusted to a mathematical response consistent of a Gaussian-Lorenztian distribution (80–20%, respectively) with a minimal χ^2 deviation.

2.3. Catalytic test

The catalytic tests were performed in a 14 mm i.d. quartz reactor. The gas (1000 ppmv NO, 1000 ppm NH_3 and 10% O_2 and Ar to balance) was forced to flow through the monolith channels by fixing the monoliths to the inner walls of the reactor using Teflon stripe. The GSVH of the performance was around 34,000 h^{-1} related to the carbon weight. The temperature reaction was set at 150, 250 and 350 °C and the reaction was allowed to proceed for 2 h until steady-state. A mass spectrometer (Balzers 422) was used to analyze the gas stream, previously calibrated with cylinders of certified known composition. The conversion of NO was calculated as follows:

$$\%\ \text{NO reduction} = \frac{(C^{i}_{NO} - C_{NO})}{C^{i}_{NO}} \times 100 \quad (1)$$

where C^{i}_{NO} is the initial concentration of NO and C_{NO} corresponds to its concentration once steady-state is reached.

3. Results and discussion

Activated carbon coated monoliths have very interesting features like a good and resistant adherence between cordierite and carbon coating, an extremely narrow and homogenous thickness of coating [22], a high-surface area and a large pore volume. The very thin carbon coating with a thickness of 600–800 nm, is a good support for SCR of NO with NH_3 reactions. In the present study, the use of liquid-phase oxidation within HNO_3, H_2SO_4 or H_2O_2 to modify the surface of activated carbon coatings is investigated. Keeping in mind the objective of introducing oxygen surface groups, which can act as anchor for a subsequently impregnation with vanadium, carbon coated monoliths have been deeply characterized after the oxidation process.

According to previous studies [29,34], acid treatments of carbon coatings have an influence in the SCR of NO with NH_3. The highest NO reduction activities fit in the middle values of fresh catalyst surface acidities. This fact points out that, the effects of acid treatments are closely related to the amount and type of functionalities created by the oxidation process. Moreover, oxidation treatments also influence in the porous structure. By the way, concentrated HNO_3, even at mild temperatures, is able to partially destroy the pore structure of activated carbon coatings as reveals the disappearing of microporous volume and the decrease of surface areas. Thus, in this study, two temperatures and oxidation times were used to oxidize activated carbon coating. Basically, as expected, shorter oxidation times or lower temperatures are favourable in terms of maintaining the pore structure. A considerable increase of oxygen surface group mass was observed after the more severe

Table 3
BET surface area and pore volumes of catalysts.

3% V wt		$V_{micro\,total}$ (cm^3/g)	$V_{micro\,(<0.7\,nm)}$ (cm^3/g)	$V_{micro\,medium}$ (cm^3/g)	$V_{mesopore}$ (cm^3/g)	S_{BET} (m^2/g)
T room 24 h	HNO_3 (c)	0.0092	0.0063	0.0029	0.0279	274
	HNO_3 2N	0.0202	0.0151	0.0050	0.0276	407
	H_2O_2	0.0172	0.0131	0.0041	0.0278	609
	H_2SO_4	0.0136	0.0099	0.0037	0.0272	456
T room 8 h	HNO_3 (c)	0.0193	0.0144	0.0049	0.0132	375
	HNO_3 2N	0.0254	0.0193	0.0061	0.0160	598
	H_2O_2	0.0167	0.0122	0.0045	0.0154	401
	H_2SO_4	0.0194	0.0136	0.0058	0.0144	524
80 °C 8 h	HNO_3 (c)	0.0169	0.0126	0.0043	0.3347	547
	HNO_3 2N	0.0204	0.0149	0.0055	0.0292	644
	H_2O_2	0.0088	0.0050	0.0040	0.0310	393
	H_2SO_4	0.0164	0.0116	0.0048	0.0190	440

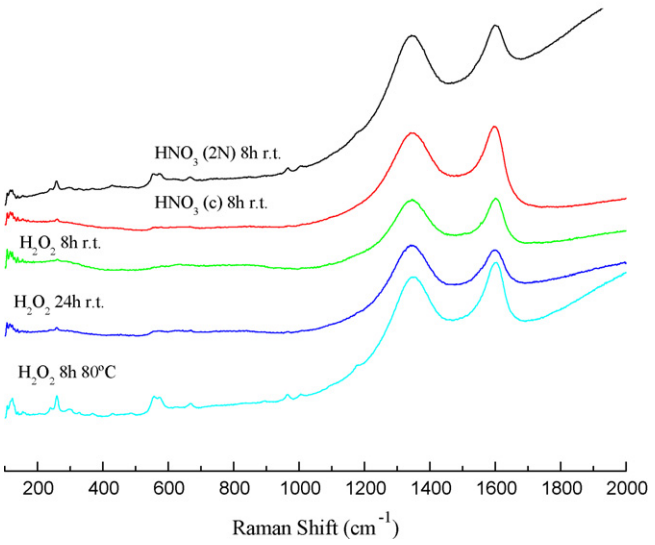

Fig. 1. Raman spectra of support oxidized with HNO_3 with different concentration and H_2O_2 with different time of oxidation and temperature.

oxidation treatments. This fact reflects the increase in the number of oxygen surface groups on the carbon frameworks after the liquid oxidation processes [30–32].

Sample BET areas and pore volumes are collected in Table 2. In general, the reduction of S_{BET} and micropore volume can be considered as a consequence of the liquid oxidation processes. It can be due to partial blockage of the micropores by some intermediates which are prone to condensate in presence of oxygen [23] or the erosion of wall pores that causes a collapse of the textural structure. According to Table 2, textural properties of activated carbon are mainly affected by the strong oxidative treatment with HNO_3. Similar results were found by Moreno-Castilla et al. [24]. Another fact that cause detrimental effect of the textural properties is the incorporation of vanadium onto the modified activated carbon coating surfaces, as indicated by the relative small but systematic decrease observed in all of them (see Table 3).

Fig. 1 shows the Raman spectra in the area of the 100–2000 cm^{-1}. For the effect of the acidic treatment, Raman spectra of support treated with HNO_3 (c), HNO_3 (2N) and H_2O_2 during 8 h at room temperature were represented. In the same figure and to study the effect of the time and the temperature of oxidation treatment in the structure, there were also included the Raman spectra of support treated with H_2O_2 during 24 h at room temperature and treated with H_2O_2 during 8 h at 80 °C.

Main crystal lattice vibration of cordierite (128, 260, 555, 578, 973, 1011, 1382 cm^{-1}) are presented in all spectra. Besides, the two typical signals of the carbon structure at 1340 and 1592 cm^{-1} are detected. The first signal is assigned to defect mode, A_{1g} (signal D) and the second associated with graphite, mode E_{2g} (signal G). The integrated intensity ratio of these two signals, D and G, in the Raman spectrum is related to graphite crystallite size (L_n) according to [37,38]:

$$L_n\,(\text{nm}) = \frac{4.4}{R} \quad \text{where} \quad R = \frac{I_D}{I_G} \tag{2}$$

Considering that both signals have similar extinction coefficients, it is possible to get the graphitic fraction according to:

$$X_G = \frac{I_G}{I_G + I_D} = \frac{1}{1+R} \tag{3}$$

The values of the graphitic fraction (X_G) for the support after oxidation treatments studied are resumed in Table 4. No variations are detected in the X_G values, and we can conclude that acidic

Table 4
Resume of carbon coating characterization parameters from Raman for support oxidized with HNO_3 with different concentration and H_2O_2 with different time of oxidation and temperature.

		I_D/I_G	L_n (nm)	X_G
HNO_3 (2N)	8 h r.t.	1.25	3.52	0.44
HNO_3 (c)	8 h r.t.	1.42	3.09	0.41
H_2O_2	8 h r.t.	1.67	2.63	0.37
H_2O_2	24 h r.t.	1.44	3.05	0.41
H_2O_2	8 h 80 °C	1.30	3.38	0.41

treatments, apparently, do not affect neither the graphitic fraction nor the carbon coating surface; though the surface functionalization could be affected, this will be described forward using other techniques as TPD and XPS.

3.1. Influence of oxidation time

Regarding the shape of N_2 sorption isotherms of activated carbon coatings before and after shorter oxidation times (not shown), oxidized activated carbon coated monoliths maintain a type IV isotherms, indicating that previous mesoporosity is still preserved. However, shorter oxidation times do not lead to a significant increase in the functionalization of carbon coatings, which is reflected by the increase of the total pore volume in comparison to longer oxidation times. In general and according to the isotherm shape, shorter time oxidations neither create a high functionalization nor destroy pore structure as longer ones do, except for concentrated HNO_3 oxidation that could even provoke a higher destruction of textural properties.

As shown in Table 2, this reduction does not have a really strong influence in the BET specific surface areas and pore volumes compare to those of longer time oxidations. Consequently, in both types of oxidations, an additional mass increase after acid treatment is observed, as revealed by the following TG measurements. TG analyses (Table 5 and Fig. 2(a) and (b)) show that decreasing oxidation time, a decrease of carbon coating mass loss that varies between 1 and 3% occurs. Only H_2O_2 oxidized sample shows an increase of mass loss. This fact can be due to the higher amount of functionalities created on the surface when shorter oxidations are carried out.

Despite of the differences caused in textural properties by both shorter and longer oxidations, it is really important to point out that, all oxidized carbon coatings essentially keep the bimodal pore size distribution, what is the main characteristic of activated carbon coatings prepared from a blend of two polymers. According to previous studies [11], the presence of micropores and mesopores is of key importance for obtaining high NO conversion; micropores enhance the dispersion of the catalyst and mesopores guarantee the accessibility to the catalyst precursor and reactants to the carbon coating inside the macropores of cordierite wall.

The reduction in functionalization concentration after shorter oxidations, but using H_2O_2 as oxidizing agent, was checked by TPD runs. Fig. 3(a) and (b) show the TPD profiles obtained for the different carbon supports. Table 6 shows the amounts of CO_2 and CO released up to 1050 °C and calculated under TPD profiles. These results show a low functionalization of the starting acti-

Table 5
Mass loss in TGA runs in (%) from the original sample.

(%)	24 h T-room	8 h T-room	8 h at 80 °C
HNO_3 (c)	12.29	11.00	10.65
HNO_3 2N	11.04	8.40	9.65
H_2SO_4	8.25	7.11	13.71
H_2O_2	5.56	9.50	9.18

Table 6
CO and CO_2 evolved from TPD runs of catalyst support after oxidation treatments.

		CO (cm^3/g)	CO_2 (cm^3/g)	CO + CO_2 (cm^3/g)	CO/CO_2
	Activated	3.3	0.4	4	7.61
24 h Troom	HNO_3 (c)	111	56	167	2.01
	HNO_3 2N	99	46	145	2.18
	H_2SO_4 2N	87	36	123	2.45
	H_2O_2	137	32	169	4.21
8 h Troom	HNO_3 (c)	66	51	117	1.30
	HNO_3 2N	76	25	101	2.98
	H_2SO_4 2N	73	13	86	5.68
	H_2O_2	118	29	147	4.00
8 h 80 °C	HNO_3 (c)	61	36	97	1.68
	HNO_3 2N	74	33	107	2.22
	H_2O_2	144	77	221	1.86
	H_2SO_4 2N	58	11	69	5.11

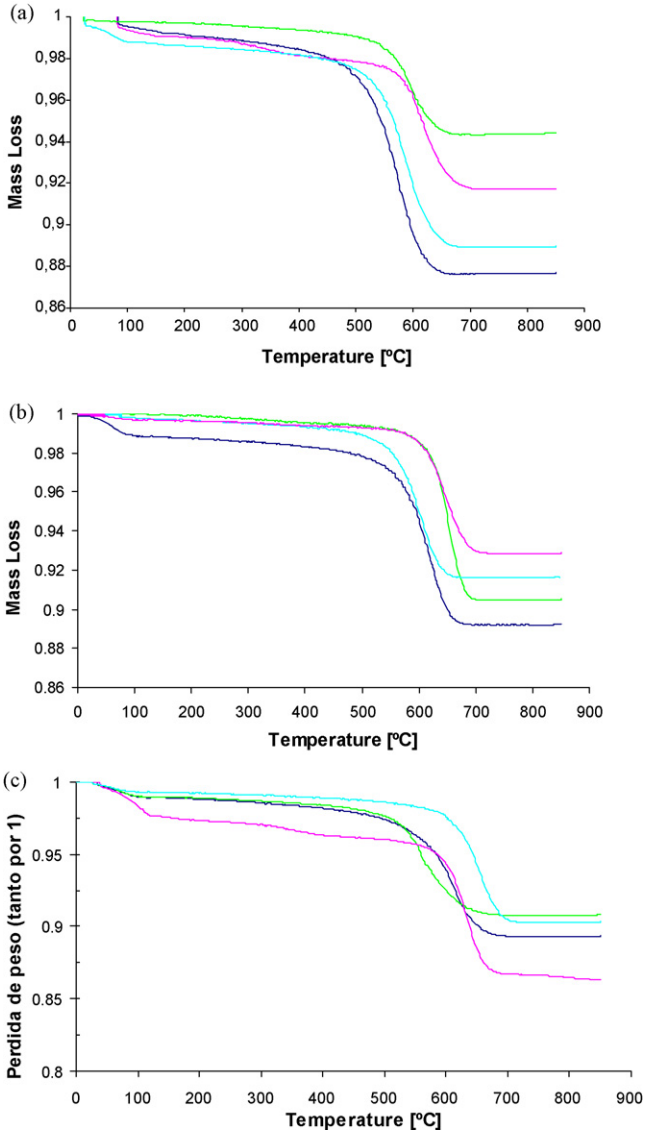

Fig. 2. TG runs of (a) supports oxidized at room temperature for 24 h, (b) supports oxidized at room temperature for 8 h and (c) (a) supports oxidized at 80 °C for 8 h. Dark blue: oxidized with concentrated HNO_3; light blue: oxidized with 2N HNO_3; green: oxidized with H_2O_2; pink: oxidized with 2N H_2SO_4. (For interpretation of the references to color in this figure legend, the reader is referred to the web version of the article.)

vated carbon. After shorter oxidative treatments, a high increase in the amount of CO and CO_2 evolving oxygen surface groups was observed. However, this increase is much lower that the increase observed after longer oxidative treatments. Shorter oxidative treatments lead to CO_2 and CO spectra with peaks and shoulders at different temperatures, mainly between 200 and 800 °C for CO_2 and 400 and 1000 °C for CO that can be attributed to different types of functionalizations as follows.

The peaks and shoulders of the TPD curves can be assigned to different functional groups depending on the temperature at which CO and CO_2 evolve [15,28]. TPD profiles were deconvoluted to assess the chemical nature of the different oxygen surface groups according to the following criteria [28]:

- four contributions have been considered in the CO profiles: carboxylic anhydrides (600–670 °C), phenols and ethers (650–700 °C), carbonyl/quinine (730–840 °C) and pyronic groups (850–1000 °C);
- the CO_2 profiles include three contributions: carboxylic acids (150–350 °C), lactones (250–350 °C) and carboxylic anhydrides (500–675 °C);
- a multiple Gaussian function was selected to fit each deconvoluted peak of TPD spectra.

The results of TPD deconvolution are summarised in Table 7. According to it, the small amount of evolved oxygen surface groups of just activated monolith and mainly released as CO at high temperature (>800 °C), can be attributed to carbonyl/quinone or even pyronic groups. This fact proves the neutral nature of the activated carbon monolith, consistent with its high value of CO/CO_2 ratio. After shorter and longer oxidative treatments, the amount of oxygen surface groups onto the activated carbon coatings was greatly increased and the ratio CO/CO_2 decreased, indicating a higher acidification of surface.

In the case of shorter HNO_3 (2N) oxidized sample, all types of evolved oxygen surface groups were significantly decreased in comparison to longer oxidized samples (up to twice the value of CO_2 evolved groups) but the kind of functionalities created are basically the same and attributed to lactone and carboxyl groups. The decrease observed in CO_2 evolved groups caused an increase of CO/CO_2 ratio that suggests a less acidic surface character of the sample. The former carboxyl groups could have been formed through condensation of close carboxylic groups formed during the oxidation treatment [28]. The lower CO/CO_2 ratio for shorter concentrated HNO_3 samples suggests the significance of the time reduction to get a more acidic surface. Concentrated HNO_3 oxidation provides a higher microporosity and a higher amount of surface oxygen groups at shorter oxidation times as reported by other authors [36] According to H_2SO_4 and H_2O_2 liquid oxidizing agents,

shorter oxidations lead to a lower acid surface character for H_2SO_4 sample and a higher acidic surface character for H_2O_2 sample. The decrease in lower temperature CO_2 evolving groups created by shorter H_2SO_4 oxidations is responsible for this change. In this case, the amount of carboxylic groups was dramatically decreased and consequently, an increase in the CO/CO_2 ratio is observed with respect to the CO/CO_2 ratio value of longer oxidized samples.

The introduction of functional groups on the carbon surface can affect the metal dispersion [33] as commented before. This phenomenon was confirmed by N_2 adsorption runs presented in Table 3. Specific BET surface area, pore diameter and pore volume were decreased after vanadia impregnation. Although reduction in pore structure parameters is not especially significant in the case of BET surface area and micropore volume, a remarkable decrease in the mesopore values can be observed and consequently also in the pore diameter. Mesopore values are reduced between 2-fold and 4-fold indicating that vanadia has been anchored onto the carbon coatings.

XPS runs were performed and resumed in Table 8. Al_{2p}, Si_{2p} signals are obtained with an average shift of around 4 eV, while

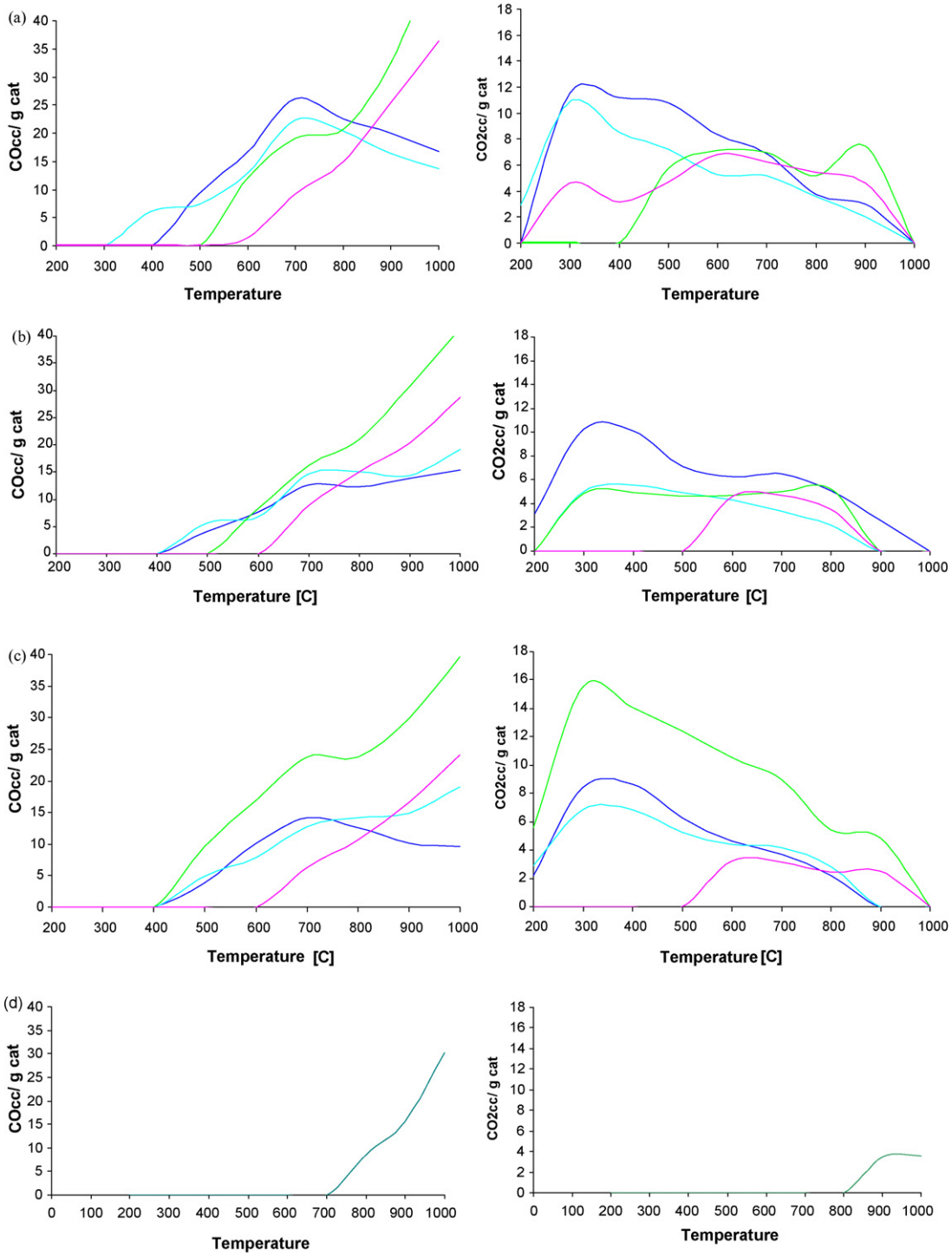

Fig. 3. TPD profiles of (a) supports oxidized at room temperature for 24 h, (b) supports oxidized at room temperature for 8 h and (c) (a) supports oxidized at 80 °C for 8 h and (d) non-oxidized supports.

C_{1s} and O_{1s} remain centred at their usual values of BE. This fact can point out that carbon is not a conductor material and consequently it avoids the appropriate transmission of the electronic beam. Going into further details, it must be said that although carbon coatings are really homogenous as reported previously in [22], it is observed differences in Si/Al and C/O ratio for the samples, suggesting the possibility of having XPS runs from areas with different thickness of carbon coating. The differences in coating thickness have to be taken into account in the following comments as not all data are provided in the same conditions. All oxidizing treatments increase the overall concentration of surface oxides, as evidenced by the increase of O_{1s}. As were described in a previous paper [38], C_{1s} peak has been fitted to four contributions related to carbon atom bonded to the following functionalities: phenols groups (ca. 286.38 eV), carbonyl groups (ca. 288.4 eV) and carboxyl groups (290.8 eV). Graphitic carbon due to non-functionalized support appears at ca. 284.8 eV with a 60–70%.

When HNO_3 (2N) was used, the BE at 286.4 eV, associated with the presence of phenolic-ether species, increases slightly, while the carbonyl and carboxyl species decrease. More significative changes are observed for treatment with concentrated HNO_3. The H_2SO_4 oxidation treatment apparently favoured the presence of less-oxidized species as carbonyl groups, while the H_2O_2 oxidation treatment favoured a more evidenced proportion of surface carboxyl groups. The time of oxidation increases the amount of functionalized carbon with the trend described for all acidic treatment.

O_{1s} peak has been fitted to two peaks with the following assignation, according to a previous work [39]: ca. 532 eV ascribed to C=O groups in phenolic, ether, ester, carbonyl groups and ca. 534–535 eV ascribed to carboxylic ones. All oxidizing treatments increase the overall concentration of surfaces oxides and a general trend is observed: time of oxidation increase the carboxylic percentage, this increment is specially observed in the case of H_2O_2.

Multiplying the relative area of O_{COOH} by the O/C atomic ratio yields the oxygen atoms in carboxylic group. Hence, dividing this value by two yields the number of carboxylic group per carbon atom is obtained. The percentage of carboxylic groups per carbon atom is included in Table 9, where it is also included for comparative purposes the CO_2/CO ratio calculated by TPD. With the exception of H_2SO_4, TPD and XPS data agree: time of oxidation increase the total amount of carboxylic groups calculated by XPS and CO_2/CO ratio calculated by TPD. The observed differences between TPD and XPS data could be due to the differences between both techniques, XPS results are limited to the surface, and these measurements have been performed in just one point of the internal plate. As a result, we expect their error to be higher.

3.2. Influence of temperature

Oxidation temperature influence is also checked in this study. Runs were performed rising temperature from room temperature to 80 °C while oxidation time remains for 8 h. Samples were characterized according to techniques reported in Section 2.2.

Once again, N_2 sorption isotherms of activated carbon coatings oxidized either at room temperature or 80 °C are type IV isotherms, indicating that mesoporosity is not destroyed (not shown here). Higher temperature oxidation leads to similar pore volumes regardless the oxidizing agent. Higher temperature oxidation does partially destroy pore structure to a greater extend than room temperature oxidation does, although in some cases, a higher micropore value is developed. What is remarkable is, that higher temperature oxidation also keeps the bimodal pore size distribution, which is characteristic of the activated carbon coatings prepared from a blend of two polymers.

The increase in the mass after higher temperature oxidation treatments is observed in the TG runs. TG analyses (Table 5 and Fig. 2(b) and (c)) showed that an increase of the oxidation temperature, causes an increase of mass loss from carbon coatings that varies between 1 and 5%. Only both HNO_3 oxidized samples show a decrease in the mass loss. This fact agrees with Bazula et al. [10] whose studies confirm that at higher oxidation temperatures (80 °C for HNO_3) the oxygen surface mass gained is smaller than at lower temperature oxidations. However, if oxidation conditions are too harsh, some carbon species are cleaved from the carbon walls. Above 400 °C, samples exhibit a higher mass loss than after room temperature oxidation, indicating that a higher funzionalized surface is created on activated carbon coatings.

Surprisingly, in our case after higher temperature oxidative treatments the amount of oxygen surface groups was not significantly increased, except for H_2O_2 treatment. Depending on the oxidizing agent, the CO/CO_2 ratio as well as TPD profile show different trends. In the case of both HNO_3 treatments, higher temperature oxidations decrease the amount of CO_2 evolving groups and consequently, an increase in the CO/CO_2 ratio is observed. In the case of H_2SO_4 oxidations, both samples exhibit similar values of CO_2 and CO evolving groups resulting therefore in a similar value of CO/CO_2 ratio what indicates the slightly influence of temperature in acidification of surface. On the other hand, H_2O_2 oxidized samples show a great increase in CO_2 evolving samples that points out that higher temperatures favour the acidification of surface.

From XPS data, resumed in Tables 8 and 9, it can be observed that the increase of the temperature in the oxidative treatment improves the amount of functionalized carbon and oxygen with a similar trend described for the influence of time of oxidation in Section 3.1; with the exception of H_2SO_4 acidic treatment, probably

Table 7
Deconvolution of TPD profiles. Total amount 100% for CO_2 and 100% for CO profile.

		Deconvolution CO_2 profile			Deconvolution CO profile			
		Carboxyl	Carboxyls	Lactone	Carboxyl anhydrides	Phenol/ethers	Carbonyl/quinone	Pyronic
24 h T room	HNO_3 (c)	25.26	29.10	45.63	9.7	22.4	67.89	–
	HNO_3 2N	23.98	36.25	39.75	24.17	25.24	50.55	–
	H_2SO_4 2N	–	16.46	66.53	–	–	18.45	81.45
	H_2O_2	–	–	68.66	–	20.23	46.65	34.90
8 h T room	HNO_3 (c)	47.8	–	52.2	41.1	21.4	–	37.6
	HNO_3 2N	15.8	–	84.2	18.8	35.6	–	25.6
	H_2SO_4 2N	36.6	–	63.4	–	17.9	45.1	37.1
	H_2O_2	–	–	100	–	32.3	–	67.7
8 h 80 °C	HNO_3 (c)	38.7	61.3	–	43.3	–	–	56.7
	HNO_3 2N	55.3	29.6	15.1	24.1	33.4	–	42.5
	H_2SO_4 2N	–	–	100	–	49.4	–	50.6
	H_2O_2	23.7	67.6	8.8	29.0	–	–	71.0

Table 8
XPS data resume.

	Relative amount (%)				Atomic ratio		Deconvolution of C_{1s} and O_{1s}	
	Si_{2p}	Al_{2p}	C_{1s}	O_{1s}	Si/Al	O/C	C_{1s}	O_{1s}
HNO_3 (c), 8 h r.t.	2.7	1.4	76.6	18.1	1.9	0.23	284.8 (60) 286.4 (25) 288.4 (10) 290.8 (5)	532.9 (60) 535.6 (40)
HNO_3 (c), 24 h r.t.	2.5	1.7	75.1	18.0	1.4	0.24	284.8 (59) 286.2 (27) 288.0 (9) 291.2 (5)	532.8 (54) 534.9 (46)
HNO_3 (c), 8 h 80 °C	3.4	0.9	77.2	17.1	3.9	0.22	284.7 (61) 286.3 (30) 288.9 (6) 290.8 (3)	532.5 (44) 534.4 (55)
HNO_3 (2N), 8 h r.t.	3.3	1.3	81.3	12.7	2.5	0.15	284.7 (60) 286.3 (19) 288.5 (16) 290.8 (5)	532.9 (62) 535.7 (38)
HNO_3 (2N), 24 h r.t.	7.3	1.5	66.2	23.5	4.7	0.35	284.8 (63) 286.3 (17) 288.4 (15) 290.9 (5)	533.0 (60) 535.8 (40)
HNO_3 (2N), 8 h 80 °C	4.0	1.0	77.3	16.5	3.7	0.21	284.8 (62) 286.3 (24) 288.5 (9) 290.8 (5)	532.9 (55) 535.8 (45)
H_2SO_4, 8 h r.t.	15.1	4.0	37.6	40.4	3.7	1.07	284.7 (60) 286.4 (15) 288.3 (21) 290.3 (5)	533.30 (55) 535.98 (46)
H_2SO_4, 24 h r.t.	14.9	1.8	47.7	34.6	7.7	0.72	284.7 (55) 286.4 (15) 288.3 (23) 290.3 (5)	532.6 (59) 535.5 (41)
H_2SO_4, 8 h 80 °C	5.2	1.36	77.8	15.1	3.8	0.19	284.7 (59) 286.3 (16) 288.6 (20) 290.9 (5)	532.6 (57) 535.3 (43)
H_2O_2, 8 h r.t.	1.7	1.2	85	11.1	1.4	0.13	284.7 (57) 296.4 (13) 288.9 (20) 290.9 (10)	532.9 (52) 535.5 (47)
H_2O_2, 24 h r.t.	3.2	1.8	77	7.1	1.6	0.09	284.7 (57) 286.3 (12) 288.9 (19) 290.9 (12)	532.5 (30) 534.3 (70)
H_2O_2, 8 h 80 °C	2.8	1.8	79	16	1.4	0.20	284.8 (55) 286.3 (11) 288.8 (19) 290.8 (15)	532.0 (18) 534.3 (82)

due to errors of the XPS technique described above. For HNO_3 (2N), the effect of the time of oxidation in the functionalization is more evident than the effect of the temperature. For H_2O_2, the oxygen functionality is specially increased after 8 h at 80 °C with a 82% of oxygen adscribed to carboxylic groups.

3.3. Catalytic activity and influence of support properties

Catalytic activity of starting and modified activated carbon coated catalysts was tested in the SCR of NO with NH_3. These materials were first placed in the bed reactor and heated up to the reaction temperature (150, 250 or 350 °C) in Ar. Once reaction temperature was reached, Argon gas was switched to the inlet gas composition and NO conversion was followed on-line in a mass spectrometer.

Significant differences were found in the catalytic activity of samples. NO conversion ratios of activated carbon coated materials treated with the different oxidation agents [29] have been reported in previous works [34]. However, to our knowledge, it has never been studied the influence of temperature and time in the oxidation process for polymeric carbon-based catalysts. This influence is studied in this section.

The effect of time reduction on catalytic activity can be observed in Fig. 4(a). Both HNO_3 oxidized samples show an opposite trend. On one hand, the catalytic activity of concentrated HNO_3 oxidized sample is greatly increased within shorter oxidation treatments. On the other hand, the catalytic activity of HNO_3 (2N) oxidized sample is slightly increase for longer oxidation treatments. Although, both trends seem to be conflicting ones, both trends agree with the new created chemistry surface. The development of an acidic surface

character is favoured by concentration and longer residence times when HNO_3 is used as liquid oxidizing agent. However, depending on the concentration longer oxidations can cause an excess in the acidity of surface that does not favour the SCR-NH_3 of NO. This fact can be due to two factors: firstly an excess of vanadium anchoring onto surface that provokes a pore blocking and avoids a high dispersion of this metal and secondly an excess in the adsorption of NH_3. NH_3 is a key reactant in the SCR that according to previous literature [5] reacts from an adsorbed-phase. If the NH_3 adsorption is excessively strong, desorption cannot properly take place in and consequently the catalytic activity of catalyst is decreased. These theories support that a too high functionalization onto the fresh surface catalyst disfavours NO conversion and this fact is observed in this work in longer concentrated HNO_3 oxidized sample behaviour. Nevertheless, a reduction of the textural properties shown in these samples may also be the cause of a poor NO conversion. A first look may suggest the existence of a pore blocking due to the higher amount of carboxylic groups that favours vana-

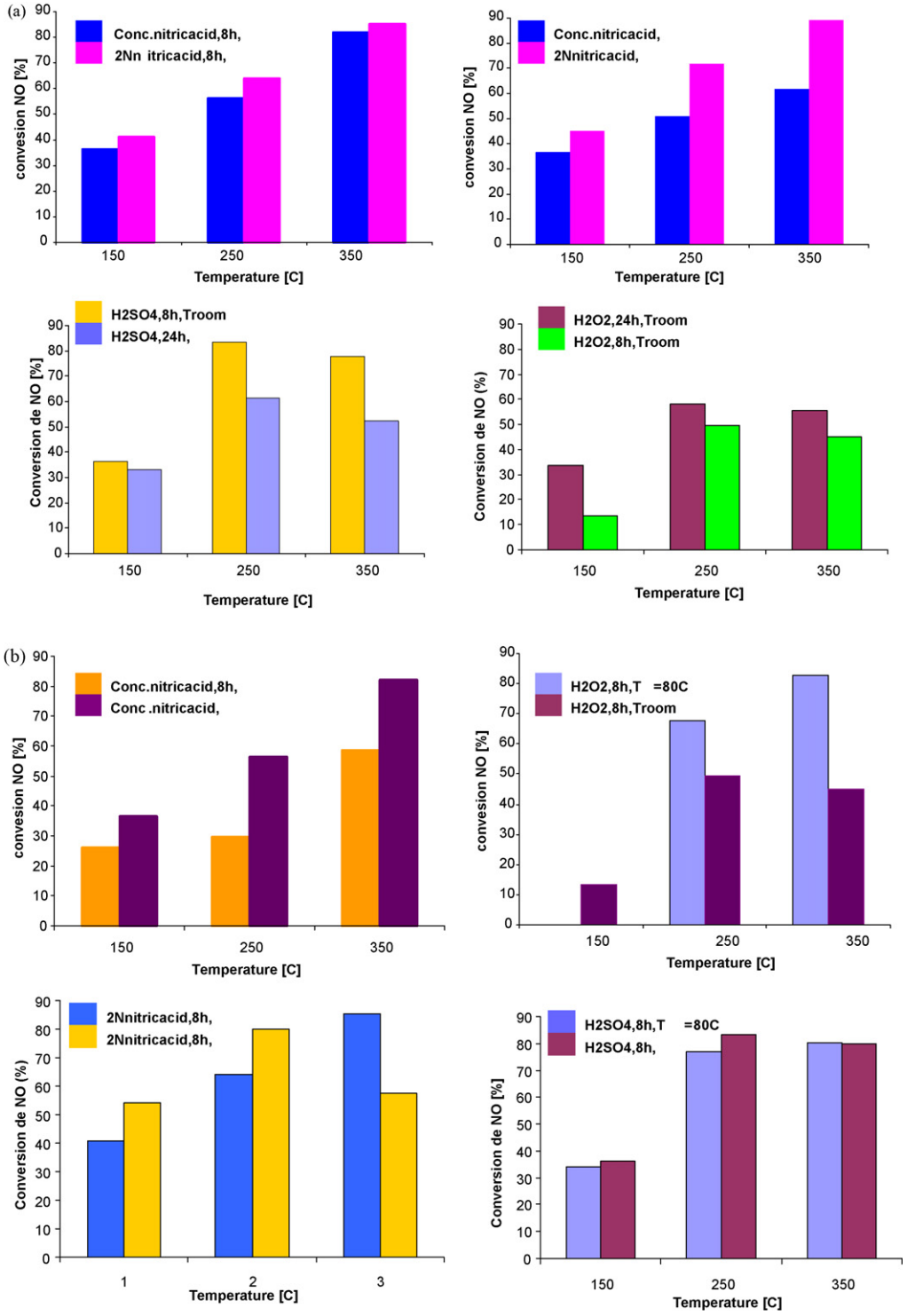

Fig. 4. NO conversion (%) at 150, 250 and 350 °C. Effect of (a) time reduction and (b) temperature increase.

Table 9
Comparison of the surface acidity obtained by means of XPS runs and TPD experiments.

	Carboxyl groups per C atom from O_{COOH} peak[a]	CO_2/CO ratio[b]
HNO_3 (c), 8 h r.t.	4.75	0.77
HNO_3 (c), 24 h r.t.	5.43	0.49
HNO_3 (c), 8 h 80 °C	6.09	0.59
HNO_3 (2N), 8 h r.t.	2.90	0.33
HNO_3 (2N), 24 h r.t.	7.12	0.45
HNO_3 (2N), 8 h 80 °C	4.90	0.45
H_2SO_4, 8 h r.t.	32.77	0.17
H_2SO_4, 24 h r.t.	14.82	0.40
H_2SO_4, 8 h 80 °C	4.17	0.45
H_2O_2, 8 h r.t.	3.06	0.04
H_2O_2, 24 h r.t.	3.20	0.23
H_2O_2, 8 h 80 °C	8.30	0.53

[a] Calculated from XPS with the formula = (% area of O_{COOH} × O/C ratio)/2.
[b] Calculated from TPD.

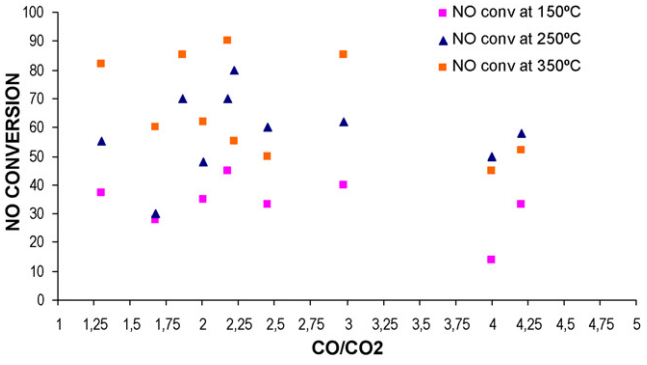

Fig. 5. Relation between NO conversion (%) and CO/CO_2 ratios.

dia anchoring onto the surface, but further investigations should be performed in this field.

H_2SO_4 oxidized sample behaves in a similar way as HNO_3 (2N) does. On the contrary, shorter H_2O_2 oxidations provide an enhancement of NO conversion. This fact can equally be related to the higher acidic character of samples, confirming that a medium-high amount of oxygen surface groups, evolved as CO_2 at lower temperatures in TPD runs is favourable to enhance NO reduction.

An increase in the oxidation temperature causes an increase in catalytic activity as long as the oxidation process is carried out with H_2O_2. H_2O_2 oxidation at higher temperature favours the creation of oxygen surface groups evolved as CO_2 at lower temperature that promotes the acidification of fresh catalyst surface. Just on the contrary, longer inorganic acid oxidative treatments reduce the NO conversion activities. In these cases, a higher temperature oxidation triggers a decrease of CO evolving groups leading to a decrease of surface acidity.

To elucidate the nature of functionalities onto fresh catalyst surface responsible for the enhancement of the catalytic activity, NO conversion has been plotted as a function of the amount of CO_2 and CO desorbed in the TPD analyses. The results exhibit (not shown here) that, even though NO conversion increases when the total amount of these groups is increased, there is no a mathematical relationship between both parameters. In general, increasing the amount of oxygen surface groups onto fresh catalyst surface to a certain extent, NO conversion activity is also increased. It is also evident that oxygen surface groups evolving as CO_2 have a greater influence on activity than those desorbing as CO, at least within the ranges studied. To evaluate the contribution of the different functionalities, the evolution of NO conversion has been related to the amounts of carboxylic acid, lactone and carboxylic anhydride groups as well as phenolic and carbonyl/quinine groups. According to both charts (not shown), it is difficult to evaluate the contribution of the different groups to the catalyst activity because a really comparable influence of all functionalities is observed.

What is clear is the fact that catalytic activity is enhanced by increasing acidity of fresh catalyst surface to a certain extent. Fig. 5 shows the relationship between the corresponding catalyst activity reached at three different temperatures and CO/CO_2 ratios. A possible explanation, previously suggested, can be achieved by correlating the NO conversion with CO/CO_2 ratios. The highest activities at each temperature are reached at around a CO/CO_2 ratio of 2.25. This fact makes understand the differences found in activity for lower temperature, shorter H_2O_2 oxidized sample (CO/CO_2 ratio of 4.00 and NO conversion at 350 °C of 45%) and lower temperature, longer HNO_3 oxidized one (CO/CO_2 ratio of 2.18 and NO conversion at 350 °C above 85%) in spite of the fact that they both present similar total amounts of $CO + CO_2$ evolving groups. In this way, it is possible to explain that lower temperature, longer HNO_3 oxidized sample and higher temperature, shorter H_2O_2 oxidized sample present a similar catalyst activity (both above 85% at 350 °C) even though the former has one and a half amount of CO and CO_2 evolving groups that the latter.

4. Conclusions

Liquid-phase oxidation by HNO_3, H_2SO_4 and H_2O_2 was used for the surface modification of carbon coated monoliths. The partial oxidation with nitric acid introduces functional groups on the carbon frameworks, which can be further anchoring places for vanadia. Lower oxidation temperatures and lower oxidation times are favourable in terms of maintaining the activated carbon coating structure. However, activated carbon coatings treated with high oxidation temperatures undergo structure transformation. It is noteworthy, that all oxidized carbon coatings keep the bimodal pore size distribution characteristic of the parent activated carbon coating, but with a decreased pore size.

The liquid oxidation treatments also modify the chemistry surface. The initial oxygen surface groups present on the activated carbon coatings and subsequently subjected to oxidation are responsible for their surface acidity. The surface groups that are desorbed as CO_2 seem to have a somewhat higher influence on the catalytic activity though all the oxygen surface groups show a beneficial effect. Shorter time oxidations increase surface acidity as long as oxidations are carried out with inorganic acids especially concentrated HNO_3. Higher temperature oxidation processes lead to a higher surface acidity as well, especially when oxidation is performed with H_2O_2.

A higher surface acidity enhance NO reduction mainly due to two facts: (1) vanadia anchoring and fixation is improved by the presence of acidic groups and (2) NH_3 adsorption is also improved as long as surface acidity increases. However, it is observed that an excess of acidity can lead to a reduction of catalytic activity because it does not allow a proper desorption of NH_3 or it promotes a higher fixation of vanadia. On one hand, NH_3 reacts from an adsorbed-phase with the gas-phase NO, so if the adsorption is too strong, desorption does not properly occur avoiding a high NO conversion. On the other hand, if vanadia is fixed in higher amount forming crystallites, the total vanadia area exposed to the catalytic reaction is reduced and consequently NO reduction is not promoted. The highest NO reductions were achieved at CO/CO_2 ratios around 2.25.

Acknowledgements

Authors thank to Spanish authorities for the financial support through the projects: Projects 437/2006.13.1 and B34/2007 (Min-

isterio de Medio Ambiente, Spain) and Project CTQ2006-09870 (Ministerio de Educacion y Ciencia, Spain). Also, we wish to thank M.C. Iritia for her contribution to the preparation and characterization of the activated carbon coatings and catalysts. A. Boyano is indebt with CSIC for her I3P pre-doctoral grant.

References

[1] M.V. Twigg, Progress and future challenges in controlling automotive exhaust gas emissions, Appl. Catal. B: Environ. 70 (2007) 2–15.
[2] I. Malpartida, M.O. Guerrero-Pérez, M.C. Herrera, M.A. Larrubia, L.J. Alemany, Catal. Today 126 (2007) 162–168.
[3] L. Castoldi, R. Matarrese, L. Lietti, P. Forzatti, Simultaneous removal of NO_x and soot on Pt–Ba/Al_2O_3 NSR catalysts, Appl. Catal. B: Environ. 64 (2006) 25–34.
[4] J. Benitez (Ed.), Process Engineering and Design for Air Pollution Control, Prentice-Hall, Englewood Cliffs, NJ, 1993, p. 254 (Chapter 6).
[5] G. Busca, L. Lietti, G. Ramis, F. Berti, Chemical and mechanistic aspects of the selective catalytic reduction of NO_x by ammonia over oxide catalysts: a review, Appl. Catal. B: Environ. 18 (1998) 1–36.
[6] G. Marbán, R. Antuña, A.B. Fuertes, Low-temperature SCR of NO_x with NH_3 over activated carbon fiber composite-supported metal oxides, Appl. Catal. B: Environ. 41 (2003) 323–338.
[7] M.F.R. Pereira, J.J.M. Orfao, J.L. Figuereiro, Oxidative dehydrogenation of ethylbenzene on activated carbon catalysts. 3. Catalyst deactivation, Appl. Catal. A: Gen. 218 (2001) 307–318.
[8] A. Boyano, M.E. Gálvez, M.J. Lázaro, R. Moliner, Characterization and kinetic study of carbon-based briquettes for the reduction of NO, Carbon 44 (2006) 2399–2403.
[9] Z. Huang, Z. Zhepping, Z. Liu, Combined effect of H_2O and SO_2 on V_2O_5/AC catalysts for NO reduction with ammonia at lower temperatures, Appl. Catal. B: Environ. 39 (2002) 361–368.
[10] P.A. Bazula, A.H. Lu, J.J. Nitz, F. Schüth, Surface and pore structure modification of ordered mesoporous carbons via a chemical oxidation approach, Micropor. Mesopor. Mater. 108 (2008) 266–275.
[11] E. García-Bordejé, L. Calvillo, M.J. Lázaro, R. Moliner, Vanadium supported on carbon-coated monoliths for the SCR of NO at low temperature: effect of pore structure, Appl. Catal. B: Environ. 50 (2004) 235–242.
[12] P. Vinke, M. Van der Eijik, M. Verbree, A.F. Voskamp, H. Van Bekkum, Modification of the surfaces of a gasactivated carbon and a chemically activated carbon with nitric acid, hypochlorite, and ammonia, Carbon 32 (1994) 675.
[13] V. Gómez-Serrano, F. Perez-Almeida, C.J. Duran-Valle, J. Pastor-Villegas, Formation of oxygen structures by air activation. A study by FT-IR spectroscopy, Carbon 37 (1999) 1517.
[14] X. Chen, M. Faber, Y. Gao, I. Kulaots, E.M. Suuberg, R.H. Hurt, Mechanisms of surfactant adsorption on non-polar, air-oxidized and ozone-treated carbon surfaces, Carbon 41 (2003) 1489.
[15] J.L. Figueiredo, M.F.R. Pereira, M.M.A. Freitas, J.J.M. Orfao, Modification of the surface chemistry of activated carbons, Carbon 37 (1999) 1379–1389.
[16] P.L. Walter Jr. (Ed.), Chemistry and Physics of Carbon, Marcel Dekker, New Cork, 1970.
[17] Z. Li, W. Yan, S. Dai, Langmuir 21 (2005) 209.
[18] K. Lászlá, K. Josepovits, E. Tombácz, Anal. Sci. 17 (2001) 1741.
[19] D. Schütch, Annu. Rev. Mater Res. 35 (2005) 209.
[20] M. Burghard, K. Balasubramaniam, Small 1 (2005) 180.
[21] L.R. Radovic, F. Rodriguez-Reinoso, Chem. Phys. Carbon 25 (1997) 243.
[22] A. Boyano, M.J. Lázaro, C. Cristiani, F.J. Maldonado-Hodar, P. Forzatti, R. Moliner, A comparative study of V_2O_5/AC and V_2O_5/Al_2O_3 catalysts for the selective catalytic reduction of NO by NH_3, Chem. Eng. J. 149 (2009) 173–182.
[23] S. Sang-Eon Park, Green approaches via nanocatalysis with nanoporous materials: functionalization of mesoporous materials for single site catalysis, Curr. Appl. Phys. 8 (2008) 664–668.
[24] C. Moreno-Castilla, F. Carrasco-Marin, F.J. Maldonado-Hodar, J. Rivera-Utrilla, Effects of non-oxidant and oxidant acid treatments on the surface properties of an activated carbon with very low ash content, Carbon 36 (1–2) (1998) 145–151.
[25] S.S. Barton, M.J.B. Evans, E. Halliop, J.A.F. McDonald, Acidic and basic sites on the surface of porous carbon, Carbon 35 (1997) 1361.
[26] P. Chingombre, B. Saha, R.J. Wakeman, Surface modification and characterisation of a coal-based activated carbon, Carbon 43 (2005) 3132.
[27] B.K. Pradhan, N.K. Sandle, Effect of different oxidizing agent treatments on the surface properties of activated carbons, Carbon 37 (1999) 1323.
[28] G.S. Szymanski, A. Karpinski, S. Biniak, A. Swiatkowski, The effect of the gradual thermal decomposition of surface oxygen species on the chemical and catalytic properties of oxidized activated carbon, Carbon 40 (2002) 2627–2639.
[29] A. Boyano, M.C. Iritia, I. Malpartida, M.A. Larrubia, L.J. Alemany, R. Moliner, M.J. Lázaro, Vanadium-loaded carbon-based monoliths for on-board NO reduction: influence of nature and concentration of the oxidation agent on activity, Catal. Today 137 (2008) 222–227.
[30] A.C. Dillon, T. Gennet, K.M. Jones, J.L. Alleman, P.A. Parilla, M.J. Heben, Adv. Mater. 11 (1999) 1354.
[31] J. Zhang, H. Zou, Q. Quing, Y. Yang, Q. Li, Z. Liu, X. Gu, Z. Du, J. Phys. Chem. B 107 (2003) 3712.
[32] Y.H. Li, S. Wang, Z. Luan, J. Ding, C. Xu, D. Wu, Adsorption of cadmium(II) from aqueous solution by surface oxidized carbon nanotubes, Carbon 41 (2003) 1057.
[33] M.A. Fraga, Y. Ding, X. JYang, L. Liu, Lin, React. Kinet. Catal. Lett. 84 (2005) 11–19.
[34] A. Boyano, M.E. Gálvez, R. Moliner, M.J. Lázaro, Carbon-based catalytic briquettes for the reduction of NO: effect of H_2SO_4 and HNO_3 carbon support treatment, Fuel 87 (2008) 2058–2068.
[36] T. Valdés-Solís, G. Marbán, A.B. Fuertes, Low-temperature SCR of NO_x with NH_3 over carbon-ceramic supported catalysts, Appl. Catal. B: Environ. 46 (2003) 261–271.
[37] M.A. Ulla, A. Valera, T. Ubieto, N. Latorre, E. Romeo, V.G. Milt, A. Monzón, Carbon nanofiber growth onto a cordierite monolith coated with Co-mordenite, Catal. Today 133–135 (2008) 7–12.
[38] M.J. Lázaro, A. Boyano, C. Herrera, M.A. Larrubia, L.J. Alemany, R. Moliner, Vanadium loaded carbon-based monoliths for the on-board NO reduction: influence of vanadia and tungsten loadings, Chem. Eng. J. 155 (1–2) (2009) 69–75.
[39] E. García-Bordejé, M.J. Lázaro, R. Moliner, P.M. Álvarez, V. Gómez-Serrano, J.L.G. Fierro, Vanadium supported on carbon coated honeycomb monoliths for the selective catalytic reduction of NO at low temperatures: influence of the oxidation pre-treatment, Carbon 44 (2006) 407–417.